HHS Public Access

Author manuscript

Dev Biol. Author manuscript; available in PMC 2018 September 01.

Published in final edited form as:

Dev Biol. 2017 September 01; 429(1): 213–224. doi:10.1016/j.ydbio.2017.06.025.

Wbp2nl has a developmental role in establishing neural and non-neural ectodermal fates

Alexander Marchak[a,1], **Paaqua A. Grant**[a,b,1], **Karen M. Neilson**[a], **Himani Datta Majumdar**[a], **Sergey Yaklichkin**[c], **Diana Johnson**[b], and **Sally A. Moody**[a,*]

[a]Department of Anatomy and Regenerative Biology, George Washington University School of Medicine and Health Sciences, Washington DC, USA

[b]Department of Biological Sciences, George Washington University, Washington DC, USA

[c]Department of Molecular and Cellular Biology, Baylor College of Medicine, Houston, TX, USA

Abstract

In many animals, maternally synthesized mRNAs are critical for primary germ layer formation. In *Xenopus*, several maternal mRNAs are enriched in the animal blastomere progenitors of the embryonic ectoderm. We previously identified one of these, *WW-domain binding protein 2 N-terminal like (wbp2nl)*, that others previously characterized as a sperm protein (PAWP) that promotes meiotic resumption. Herein we demonstrate that it has an additional developmental role in regionalizing the embryonic ectoderm. Knock-down of Wbp2nl in the dorsal ectoderm reduced cranial placode and neural crest gene expression domains and expanded neural plate domains; knock-down in ventral ectoderm reduced epidermal gene expression. Conversely, increasing levels of Wbp2nl in the neural plate induced ectopic epidermal and neural crest gene expression and repressed many neural plate and cranial placode genes. The effects in the neural plate appear to be mediated, at least in part, by down-regulating *chd*, a BMP antagonist. Because the cellular function of Wbp2nl is not known, we mutated several predicted motifs. Expressing mutated proteins in embryos showed that a putative phosphorylation site at Thr45 and an α-helix in the PH-G domain are required to ectopically induce epidermal and neural crest genes in the neural plate. An intact YAP-binding motif also is required for ectopic epidermal gene expression as well as for down-regulating *chd*. This work reveals novel developmental roles for a cytoplasmic protein that promotes epidermal and neural crest formation at the expense of neural ectoderm.

Keywords

foxd3; zic2; PAWP; placodes; neural crest; neural plate

*Corresponding author: Dr. Sally A. Moody, Department of Anatomy and Regenerative Biology, George Washington University School of Medicine and Health Sciences, 2300 I Street, NW, Washington, DC, 20037, USA, V: 1-202-994-2878, F: 1-202-994-8885 samoody@gwu.edu.

[1]these authors contributed equally

Introduction

One of the earliest decisions in embryonic development is the formation of the three primary germ layers, and in many animals maternally synthesized mRNAs are critical for their formation. Although the embryonic ectoderm is sometimes considered a “default” germ layer because in explant culture it will develop in the absence of external signaling factors (Itoh and Sokol, 2014), it is not simply a passive fate choice in the intact embryo. In *Xenopus*, for example, there are maternal factors sequestered in the animal blastomeres that promote the embryonic ectoderm by repressing mesoderm and endoderm formation (Itoh and Sokol, 2014; Zhang and Klymkowsky, 2007). In a microarray screen for maternal mRNAs enriched in animal blastomere progenitors of the ectoderm we identified *WW-domain binding protein 2 N-terminal like* (*wbp2nl*), which is maternally deposited in all four animal blastomeres, and is zygotically expressed in the animal cap ectoderm of the blastula, the embryonic ectoderm and involuting mesoderm of the gastrula, and the neural ectoderm, border zone, and dorsolateral epidermis in the neural plate stage embryo (Grant et al., 2014). This expression pattern suggests that Wbp2nl may be involved in specifying the ectoderm germ layer and/or its three derivatives: non-neural (future epidermis), border zone (future neural crest and cranial placodes) and neural (future neural plate).

Wbp2nl, also known as Peri-Acrosomal WW-domain binding Protein (PAWP), belongs to a large family of WW-domain binding proteins (WWbps) whose members are involved in a variety of cellular processes crucial for cell fate decisions, including signal transduction, protein stability, and regulation of RNA polymerase activity (Hofmann and Bucher, 1995; Sudol et al., 2001). WWbp’s contain variable length proline-rich regions that bind to the WW-domains of other proteins, many of which have crucial roles in developmental signaling pathways (Salah et al, 2012; Sudol, 2012). Previous work showed that Wbp2nl is present in the peri-acrosomal region of the sperm of several vertebrates (bull, mouse, rat, pig, rabbit, *Xenopus*), and is required for egg activation by eliciting intracellular calcium release (Aarabi et al., 2010; Wu et al., 2007). However, the role of egg- and/or zygote-derived Wbp2nl in embryonic development has not been described.

In this study we assessed the developmental role of Wbp2nl using loss- and gain-of-function analyses. We show that Wbp2nl is involved in establishing the relative sizes of the neural plate, border zone, and epidermis territories that are derived from the embryonic ectoderm (Groves and LaBonne, 2014). The effects in the neural plate are mediated, at least in part, by down-regulating the expression of *chd*, a BMP antagonist. Bioinformatics analyses revealed numerous putative functional sites in the PH-G and WWbp domains of Wbp2nl. Mutation of some of these sites show that the putative phosphorylation of Thr45 as well as preservation of an α-helical structure in the PH-G domain are required for the protein to ectopically induce *K81, foxd3* or *zic2* in the neural plate; a YAP-binding motif in the WWbp-domain is required for ectopic *K81* expression as well as efficient *chd* repression. This first description of an embryonic role for Wbp2nl shows that it is required for the division of the ectodermal germ layer into its functional domains.

Materials and methods

Obtaining embryos and microinjections

Wild type, outbred *Xenopus laevis* embryos were obtained by gonadotropin-induced natural mating of adult frogs, as previously described (Moody, 2000). Embryos were picked at the 2-cell stage, when the first cleavage furrow bisects the lightly pigmented region of the animal hemisphere, to facilitate identification of the cardinal axes (Klein, 1987; Miyata et al., 1987). This ensures accurate identification of the dorsal and ventral animal blastomeres with predominantly neural versus predominantly epidermal developmental fates (Moody and Kline, 1990). When selected embryos reached 8-cells, the dorsal-animal (D1) or the ventral-animal (V1) blastomere was microinjected with mRNA or antisense Morpholino oligonucleotides (MOs) as described elsewhere (Moody, 2000).

Blastomere explants

Both ventral animal blastomeres were injected with *wbp2nl* mRNA, and upon completion of the next cell cycle, both midline daughters (16-cell V1.1 blastomeres, Moody 1987) were dissected free and cultured as explants, as previously described (Grant et al., 2013; Gaur et al., 2016). When sibling controls reached neural plate stages, explants were fixed and processed for in situ hybridization as described below.

Construction of Wbp2nl constructs

To make a morpholino-sensitive mRNA, *Xenopus laevis wbp2nl* was obtained (Open BioSystems; BC082812.1) and the ORF plus 66 base pairs of its 5' UTR region generated by PCR using standard procedures and cloned into the ClaI/XhoI sites of the pCS2$^+$ vector (*pCS2$^+$-wbp2nl*). To make a morpholino-resistant mRNA, the ORF was generated by PCR and cloned into the EcoRI/XhoI sites of a pCS2$^+$ vector containing a 5' Myc-tag (*pCS2$^+$-5'MT-wbp2nl*). Mutations were introduced into the *pCS2$^+$-wbp2nl* plasmid with the QuikChange Lighting Site-Directed Mutagenesis kit (Agilent). *wbp2nl-T45A* was constructed by a one-nucleotide base change (ACA to GCA) resulting in T45A conversion, replacing a predicted serine/threonine kinase phosphorylation site. *wbp2nl-Y55F* was constructed by a one-nucleotide base change (TAC to TTC) resulting in Y55F conversion, replacing a predicted site of tyrosine kinase phosphorylation. *wbp2nl-Y91G* was constructed by changing two nucleotides (TAC to GGC) resulting in Y91G conversion. This mutation replaced a predicted site of tyrosine phosphorylation. *wbp2nl-F127P* was constructed by changing two nucleotides (TTC to CCC) resulting in F127P conversion predicted to disrupt the α-helix C-terminal to the PH-G domain. *wbp2nl-Y282F* was constructed by a one-nucleotide base change (TAC to TTC) resulting in Y292F conversion in the YAP binding motif (PPPY to PPPF), eliminating a predicted phosphorylation site. In addition, an HA tag was added to the 3' end of the *wbp2nl* open reading frame in *pCS2$^+$-wbp2nl* using the same mutagenesis kit. All constructs were fully sequenced in both directions.

In vitro synthesis of mRNAs and antisense RNA probes

mRNAs were synthesized *in vitro* (mMessage mMachine kit; Ambion). They were mixed with nuclear-localized *β-galactosidase (nβ-gal)* mRNA as a lineage tracer (100pg/nl) at the

indicated concentrations: wild type *wbp2nl* (200pg/nl; 400pg/nl), *wbp2nl-T45A* (400pg/nl), *wbp2nl-Y55F* (400pg/nl), *wbp2nl-Y91G* (400pg/nl), *wbp2nl-F127P* (400pg/nl), and *wbp2nl-Y282F* (400pg/nl). Antisense RNA probes for *in situ* hybridization (ISH) were synthesized *in vitro* (MEGAscript kit; Ambion) as previously described (Sullivan et al., 2001; Yan et al., 2009).

Antisense oligonucleotide morpholino design and validation

To knock-down endogenous levels of Wbp2nl protein in the embryo, two translation-blocking MOs that target both homeologues were purchased (Gene-Tools, LLC) (Supplemental Fig. 2). An equimolar mixture of *wbp2nl* MOs (9.0ng per blastomere) was microinjected into one dorsal and one ventral blastomere on one side of the 8-cell embryo. Both MOs were lissamine labeled so that cells in the embryo in which knock-down was achieved could be identified. To verify the ability of the MOs to block *wbp2nl* translation, *Xenopus* oocytes were injected with 9ng of the MO cocktail and with either 2ng of *wbp2nl-3'HA* mRNA (*pCS2*$^{+}$*-wbp2nl* construct contains 66 bp of *wbp2nl* 5'UTR = MO sensitive) or 2ng of *5'MT-wbp2nl* mRNA (rescue mRNA). The latter is MO-resistant because there is no *wbp2nl* 5' UTR present and 6 copies of the Myc-tag epitope sequence precede the *wbp2nl* ORF (Supplemental Fig. 2). The oocytes were cultured overnight at 18°C, lysates prepared and Western blotting performed with an HA-tag or Myc-tag antibody as previously described (Neilson et al., 2012) (Supplemental Fig. 3A, B). In addition, the reversal of the MO knock-down phenotype in whole embryos was demonstrated by injecting 400pg of rescue mRNA (*5'MT-wbp2nl*) immediately after embryos were injected with 2.25ng of the MO cocktail (Supplemental Fig. 3A, B).

Whole embryo in situ hybridization

Embryos were cultured to gastrula (st. 10.5–11.5), neural ectoderm (st. 12–14) or neural plate (st. 16–18) stages (Nieuwkoop and Faber, 1994), fixed in 4% paraformaldehyde (in 0.1M MOPS, 2mM EGTA Magnesium, 1mM $MgSO_4$, pH 7.4), stained for β-Gal histochemistry if injected with mRNAs, and processed for in situ hybridization (ISH) as previously described (Yan et al., 2009). Embryos were first scored for presence of lineage marker (lissamine-labeled MOs or nβ-Gal for mRNA) to demonstrate a successful injection. Then, position, intensity and size of the expression domain were compared on the injected, lineage-labeled side to the control, uninjected side of the same embryo as a control for inter-embryo variation. Samples were derived from at least three different clutches of eggs from three different sets of outbred, wild type parents. Samples were scored independently by two authors (AM, PG, or SAM). Frequencies of an observed phenotype in two different experimental groups were compared by Chi-squared statistical analysis. Sizes of gene expression domains were compared to control sides of the same embryo by the paired t-test.

Immunostaining

Because we could not identify a commercial antibody that recognizes the *Xenopus* protein, a dorsal-animal blastomere was injected with *myc*-tagged *wbp2nl* mRNA (50pg). Embryos were fixed at stage 14, cryosectioned, and immunostained with an anti-Myc antibody (#9B11, Cell Signaling) as previously described (Neilson et al., 2012). Images were collected using a Zeiss LSM 710 confocal system as previously described (Neilson et al.,

2012; Klein et al., 2013). To assay for BMP signaling, embryos were injected with cytoplasm-localized *β-galactosidase (cβ-gal)* mRNA (controls) or *wbp2nl + cβgal* mRNAs. When embryos reached stages 11–12, they were fixed and processed for whole mount immunostaining using an anti-phosphorylated SMAD 1/5/8 antibody (#9511, Cell Signaling) as previously described (Neilson et al., 2012).

Prediction of identity, structure and potential functional domains/motifs

Alignments of *Xenopus* and human sequences were done with Clustal Omega (Sievers et al., 2011) and MUSCLE (Edgar, 2004) and displayed using ESPript (Xavier et al., 2014). Trees were prepared using MRBAYES (Huelsenbeck and Ronquist, 2001; Dereeper et al., 2008). Secondary structure was predicted at the Porter (http://distill.ucd.ie/porter/; Pollastri and McLysaght, 2005), Psipred (http://bioinf.cs.ucl.ac.uk/psipred/; Buchan et al., 2013; Jones, 1999) and nps@ (npsa-pbil.ibcp.fr) websites. Modeling of the tertiary structure was conducted at the Phyre 2 server (sbg.bio.ic.ac.uk/phyre2; Kelley et al., 2015). Wbp2nl was analyzed for a nuclear localization signal (NLS) using cNLS (nls-mapper.iab.keio.ac.jp/; Kosugi et al., 2009) with a cut-off score 2.0–7.0, and with an algorithm based Markov–hidden model (moseslab.csb.utoronto.ca; Nguyen Ba et al., 2009). Prediction of a mitochondrial export signal was conducted at (ihg.gsf.de/ihg/mitoprot.html; Claros and Vincens, 1996). Prediction of subcellular localization was conducted at (wolfpsort.hgc.jp; Horton et al., 2007). Putative motifs were analyzed at The Eukaryotic Linear Motifs Resource for Functional Sites in Proteins (elm.eu.org; Dinkel et al., 2016). Annotation of functional and structural domains was conducted at SMART (smart.embl-heidelberg.de; Letunic et al., 2015).

RESULTS

Prediction of identity, structure and cellular localization of Wbp2nl

Phylogenetic tree analysis of a collection of vertebrate Wbp2 and Wbp2nl proteins separates each gene into a separate clade (Supplemental Fig. 1), although protein sequences showed high variability. A pairwise comparison of the amino acid identities across taxa (not shown) indicates that the mammalian Wbp2nl proteins segregate from the *Xenopus* (and other non-mammalian taxa) versions due to several insertions not found in either *Xenopus* species (*laevis, tropicalis*) Wbp2nl or Wbp2 proteins, suggesting that the human version of this gene diverged during mammalian evolution. Clustal analysis (Sievers et al., 2011) to determine the amino acid sequence homology between human and *Xenopus* Wbp2-related proteins is consistent with the tree analysis. The sequence of *Xenopus* Wbp2nl (291aa) is more similar to *Homo sapiens* WBP2 (261aa; 68% conserved) (Fig. 1A) than to *Homo sapiens* WBP2NL (309aa; 52% conserved) (Fig. 1B).

Because the cellular function of Wbp2nl is not known, we undertook a bioinformatics approach to predict structural characteristics. Prediction of secondary structure with various algorithms indicates that Wbp2nl contains two highly conserved domains: a highly structured Pleckstrin Homology-GRAM (PH-G) domain and a highly unstructured WW-domain binding domain (WWbp) (Fig. 1A). The PH-G domain of *Xenopus laevis* is 62% identical and 78% conserved compared to human WBP2, and the *Xenopus laevis* WWbp

domain is 55% identical and 59% conserved compared to human WBP2 (Fig. 1A). Since the tertiary structure of the PH-G domain has been solved in several PH-G-containing proteins (Begley et al., 2003), tertiary structure of PH-G in Wbp2nl was modeled as described (Kelley and Sternberg, 2009; Kelley et al., 2015). The modeled PH-G domain has ~7 β-strands (the number depending upon the prediction program used) forming two β-sheets followed by a characteristic, highly conserved α-helix (Fig. 1A); it is highly similar to that of the PH-G domains of MTMR2 and pleckstrin (Begley et al., 2003), but is less compact and has a protruding loop between **(**β-strands *6* and *7*. The WWbp domain contains two PPXY motifs (219–222aa; 279–282aa) that can bind to other proteins containing a WW domain.

Although the PAWP protein is reported to be peri-acrosomal (Wu et al., 2007), the subcellular localization of Wbp2nl in embryonic cells has not been determined. Therefore, the protein sequence was analyzed for the presence of subcellular localization signatures by several algorithms. None detected a nuclear localization signal or a mitochondrial export signal. A method by Horton et al. 2007) predicted predominantly cytoplasm localization and no trans-membrane allocation (no N-terminal signal peptide). This algorithm and the ELM predicted an endoplasmic reticulum retention signal (KKXX) at the C-terminus, and two motifs (YRVI, 55–58 aa; YMPM, 273–276 aa) are predicted to interact with the μ-subunit of heterotetrameric adaptor protein (AP) complexes for clathrin mediated vesicular transport. Together these analyses indicate that Wbp2nl is likely to be predominantly a cytoplasmic protein. This was confirmed by immunostaining for an expressed Myc-tagged version of Wbp2nl (Fig. 1C). Staining was perinuclear as well in cytoplasmic tubular patterns, both of which are consistent with endoplasmic reticulum.

Decreasing Wbp2nl levels expands the neural plate

Because maternal *wbp2nl* mRNA is enriched in animal blastomeres (Grant et al., 2014), we investigated whether loss of the Wbp2nl protein in this region would impact the development of the embryonic ectoderm and/or its later segregation into neural, neural border zone and epidermal domains. This was accomplished by microinjecting translation blocking antisense morpholino oligonucleotides (MOs) complimentary to two 5' sites in the *wbp2nl* mRNA (Supplemental Fig. 2) into blastomere progenitors of the ectoderm in the 8-cell embryo (Fig. 2A). The efficacy and specificity of the *wbp2nl* MOs were biochemically confirmed (Supplemental Fig. 3) in accord with published standards (Blum et al., 2015).

Reducing Wbp2nl levels in the dorsal-animal blastomere (D1; Fig. 2A), which targets knock-down to the neural ectoderm (Moody and Kline, 1990), decreased the *sox2* expression in the neural ectoderm in the majority of embryos; it caused a reduction of other neural ectodermal genes (*foxd4l1, sox11, zic1, zic2*) at much lower frequencies (Fig. 2B). These results suggest that the reduced levels of Wbp2nl achieved in the morphants does not prevent neural induction, but may delay the formation of *sox2*-positive neural plate stem cells. Consistent with this interpretation, by neural plate stages the expression domains of neural genes were expanded in most embryos (Fig. 2C). Measuring the width of the neural plate prior to elevation of the neural folds confirmed significant expansion of the domains of *sox2* (21.50 vs. 14.75, $p<0.001$); *sox11* (15.39 vs. 11.14; $p<0.001$), *zic1* (20.07 vs. 14.93;

p<0.001), and *zic2* (17.26 vs. 13.21; p<0.001) compared to the control side of the same embryo. In spite of the size differences between control and experimental sides of the morphant embryos, the neural tube successfully closed, indicating that the expanded neural plate domain was not simply a failure of neural fold elevation.

In contrast, knock-down of Wbp2nl diminished the expression domains of several neural crest (*pax3, tfap2a, foxd3, zic1, zic2*) and two cranial placode (*six1, sox11*) genes (Fig. 2C, D). Interestingly, however, the expression of *foxi1* in the PPE was rarely affected (Fig. 2E). These results indicate that Wbp2nl is necessary for the expression of many border zone genes. To determine whether Wbp2nl also is necessary for epidermal gene expression, we targeted knock-down to the ventral-animal blastomere progenitor of the epidermis (V1; Fig. 2A; Moody and Kline, 1990). This caused a loss of *tfap2a* and epidermal keratin (*K81*) expression in the gastrula animal cap ectoderm and later in the ventral epidermis, but the animal cap expression of *foxi1* rarely was affected (Fig. 2E). Although we expected that the loss of epidermal genes in the ventral ectoderm would result in ectopic neural plate gene expression, this was never observed (*sox2*, n=33; *foxd4l1*, n=78; *sox11*, n=51; *zic2*, n=19). The continued expression of *foxi1* after Wbp2nl knock-down (Fig. 2E) might prevent these cells from converting to neural. Together, these results demonstrate that reducing Wbp2nl in the dorsal ectoderm expands the neural plate domain at the expense of the border zone, and reducing Wbp2nl in the ventral ectoderm represses some but not all epidermal genes.

Increasing Wbp2nl levels causes ectopic epidermal and neural crest gene expression

The loss-of-function experiments predict that Wbp2nl preferentially promotes epidermal and neural crest gene expression. To test this, *wbp2nl* mRNA was microinjected into the dorsal-animal blastomere (Fig. 2A) to target gain-of-function (GOF) to the neural ectoderm (Moody and Kline, 1990). This resulted in ectopic induction of *K81* in the neural ectoderm of the gastrula (Fig. 3A); this response was transient, as it was infrequently observed at neural plate stages (Fig. 3A). In contrast, *foxi1* rarely was induced in the gastrula neural ectoderm (Fig. 3B). Wbp2nl GOF also caused ectopic induction of two neural crest genes (*foxD3, zic2*) in the majority of the embryos at both gastrula and neural plate stages (Fig. 3C, D). Surprisingly, border zone genes that are required for neural crest formation (*pax3*, n=43; *tfap2a*, n=42; *zic1*, n=53) were not ectopically induced (Fig. 3E, F). Consistent with reports that *zic1* is required for placode gene expression (Hong and Saint-Jeannet, 2007; Jaurena et al., 2015), in no case was ectopic neural plate expression of *six1* detected (Fig. 3G). In line with the expression of epidermal and neural crest genes in the neural ectoderm, some neural plate genes (*zic1, sox2, sox11, irx1*) were down-regulated by Wbp2nl (Fig. 3F, I, J, K, M). Interestingly, expression of another neural plate gene, *foxD4l1* (aka *foxD5*, Sullivan et al., 2001), which acts upstream of *sox2, sox11* and *irx1* (Yan et al., 2009; Moody et al., 2013), was unaffected (Fig. 3H), suggesting that Wbp2nl affects neural plate gene expression downstream of *foxD4l1* activity. Finally, when the Wbp2nl-expressing clone overlapped with the border of the neural plate, some border zone genes were unaffected (*pax3*, n=43; *tfap2a*, n=42), whereas *zic1* and cranial placode genes (*six1, irx1, sox11*) were down-regulated (Fig. 3F, J, K, L, M). Together, these results indicate that increased levels of Wbp2nl in the dorsal ectoderm promote ectopic epidermal and neural crest gene expression,

and concomitantly repress neural plate and cranial placode gene expression, consistent with the results of the loss-of-function experiments (Fig. 2).

Does Wbp2nl affect other germ layers?

Since *wbp2nl* mRNA is maternally expressed, we assessed whether it affects germ layers other than the ectoderm. We did not detect *wbp2nl* expression in the embryonic endoderm (Grant et al., 2014), and altering its levels did not change endoderm gene expression. Wbp2nl knock-down did not affect the expression domains of *sox17* or *edd* (Fig. 4A, B). Likewise, increased levels of Wbp2nl neither ectopically induced nor altered their endogenous domains (Fig. 4A, B). In contrast, *wbp2nl* is expressed in the dorsal involuting mesoderm and later in paraxial mesoderm (Grant et al., 2014). Thus, some of the effects on ectoderm genes might result from altering dorsal mesoderm gene expression. To test this, we examined the expression of a pan-mesodermal T-box gene, *bra*, and a dorsal mesoderm gene encoding a secreted anti-BMP factor, *chd*. Loss of Wbp2nl in the dorsal-animal lineage resulted in reduced expression of both genes in low percentages of embryos at gastrula stages, whereas by neural plate stages their expression domains were slightly broader in a low number of embryos (Fig. 4C, D). Increased Wbp2nl levels had no discernable effect on *bra* expression, but repressed *chd* in the majority of embryos (Fig. 4C, D). Thus, with the exception of the Wbp2nl dorsal GOF repression of *chd*, the effects on mesoderm are minimal, suggesting that Wbp2nl does not alter mesoderm germ layer formation per se.

We hypothesized that the reduction in *chd* along the dorsal midline, which is predicted to locally increase BMP4 signaling, might be responsible for the Wbp2nl GOF-induced ectopic expression of epidermal and neural crest genes within the neural plate. To test this, we co-injected 400pg *wbp2nl* mRNA with 20pg of *chd* mRNA in the dorsal-animal blastomere. The frequency of ectopic induction of *K81* was nearly eliminated (from 90.2 to 4.3%, n=23; $p<0.005$), and those of *foxd3* (from 100 to 55.0%, n=44, $p<0.005$) and *zic2* (from 86.2 to 60.6%, n=23, $p<0.05$) were significantly reduced; when induction occurred, it was very weak (compare Fig. 5A to Fig. 3A, C, D). These results suggest that one developmental activity of Wbp2nl in the dorsal ectoderm is to increase BMP signaling by down-regulating *chd* expression. In support of this, we immunostained embryos for the nuclear localization of phosphorylated SMAD1/5/8, which indicates a response to BMP signaling. In embryos in which nuclear staining was detected in the ventrally located BMP signaling center (as a positive control for the immunolocalization; Fig. 5B–b), embryos injected only with lineage tracer did not show nuclear staining in the neural plate (Fig. 5B–a). In contrast, more than half of embryos injected with *wbp2nl* mRNA displayed nuclear staining in the neural plate (Fig. 5B–c).

These results predicted that expressing *wbp2nl* mRNA in the ventral-animal blastomere (Fig. 2A) would locally increase epidermal gene expression, but neither *foxi1* (n=25) nor *K81* (n=20) were detectably affected. However, two neural crest genes (*foxd3, zic2*) were ectopically induced (Fig. 5C). To test whether Wbp2nl is sufficient to induce neural crest genes in naïve epidermal progenitors, we injected ventral-animal blastomeres with *wbp2nl* mRNA and explanted their 16-cell midline daughters (V1.1; Moody, 1987) into a simple salt medium. When cultured to neural plate stages, control, uninjected blastomere explants never

expressed *foxd3* or *zic2*, whereas Wbp2nl-expressing ventral blastomere explants all expressed these two genes (Fig. 5D). These results suggest that in the ventral epidermis, increasing Wbp2nl either sufficiently reduced BMP signaling to allow neural crest gene expression, or acts via a BMP-independent mechanism.

Which motifs in Wbp2nl are required for its effects on embryonic gene expression?

Our search to identify potential functional domains and motifs in Wbp2nl found 28 motifs that predicted possible interactions with 99% confidence ($p < 0.01$; Supplemental Fig. 4). The majority of motifs are within the PH-G and WWbp domains, and can be broadly categorized into three types: 1) serine/threonine kinase recognition motifs; 2) Scr Homology (SH)-domain interaction motifs; and 3) WW-domain interaction motifs. To reveal putative functional motifs that may be relevant to the gene expression phenotypes we observed after increasing the levels of wild type (wt) protein (Fig. 3), we mutated several sites.

Putative serine/threonine kinase recognition motifs are found at several sites in Wbp2nl, most of which are clustered within the PH-G domain (Supplemental Fig. 4). Since three putative kinase sites (GSK, NEK, PKA2) converge on Thr45, which in a 3-D model of the PH-G domain lays in a groove between the two β-sheets, is oriented to the solvent, and is therefore accessible for possible phosphorylation, we changed this site to alanine (Wbp2nl-T45A; Fig. 1A). There is a motif (FLTAYRVI, 51–58aa) that is similar to an immunoreceptor tyrosine-based switch motif (ITSM) ($p<0.005$); phosphorylation of the tyrosine residue in this motif plays an important role in interactions with SH2-containing adaptor molecules (Sidorenko and Clark, 2003). Therefore, we changed the tyrosine to phenylalanine (Wbp2nl-Y55F; Fig. 1A). There is a STAT5 SH2 motif (YIKG; 91–94 aa) in the highly conserved central portion; we changed the tyrosine to a glycine (Wbp2nl-Y91G; Fig. 1A). Of these phosphorylation site mutants, only Wbp2nl-T45A showed significantly less ectopic expression of *K81* and *foxd3* compared to wt Wbp2nl (Fig. 6A). Interestingly, the Wbp2nl-Y55F mutation caused stronger and broader ectopic staining of *foxD3*, and the Wbp2nl-Y91G mutation caused stronger and broader ectopic staining of *zic2* (Fig. 6B; compare to wt protein in Fig. 3C, D). The Wbp2nl-T45A mutation also significantly reduced the ability of the protein to repress *sox11* neural plate expression (Fig. 6C), but had no effect on *irx1* neural plate or placode gene expression (Fig. 6D) or on *chd* expression (Fig. 6E). The only phenotype altered by the Y55F mutation was a reduction in its ability to repress *irx1* in the neural plate (Fig. 6C). The Y91G mutation caused a reduction in its ability to repress *irx1* in the neural plate and the placodes (Fig. 6C, D). These results indicate that each putative phosphorylation site plays a subtly different role in the ability of Wbp2nl to ectopically induce or repress ectodermal genes, and none plays a role in repressing *chd*.

Because an α-helix at the C-terminal end of the PH-G domain is conserved across WWbp-containing proteins, we disrupted this structure by changing a phenylalanine to proline (Wbp2nl-F127P; Fig. 1A). This mutation significantly interfered with the ability of the protein to ectopically induce *K81, foxd3* or *zic2* in the neural plate (Fig. 6A); in the few embryos that still displayed ectopic expression, it was weak. The F127P mutation also significantly reduced the repression of *sox11* in the neural plate and of both *sox11* and *irx1* in the placodes (Fig. 6C, D). In contrast, it had no effect on *chd* repression (Fig. 6E). These

results suggest that the α-helix in the PH-G domain likely provides a 3-dimensional conformation that enables Wbp2nl to ectopically induce epidermal and neural crest genes and repress neural plate or placode genes.

Wbp2nl contains a WW-domain interaction motif (PPPY; 279–282 aa; Fig. 1A) that is recognized by Group I WW-domains. In PAWP this motif interacts with the ubiquitin ligase Nedd4 and the Hippo pathway component YAP (Wu et al., 2007). We changed the tyrosine phosphorylation site in this motif to phenylalanine to interrupt YAP binding (Wbp2nl-Y282F; Fig. 1A). This mutation nearly eliminated the ability of Wbp2nl to ectopically induce *K81* in the neural plate, had only a mild effect on *foxd3*, and had no significant effect on *zic2* ectopic expression (Fig. 6A). Wbp2nl-Y282F also reduced *sox11* neural plate and placode expression, but not *irx1* expression (Fig. 6C, D). The Y282F mutation also reduced, but did not eliminate, the frequency of *chd* repression (Fig. 6E). These results suggest that YAP binding likely plays a key role in the ectopic expression of *K81* in the neural plate, and contributes to the neural plate repression of *sox11* but not *irx1*. It is the only mutation we tested that reduced the incidence of *chd* repression.

DISCUSSION

In many animals maternally synthesized mRNAs are critical for the formation of the primary germ layers. We previously identified maternal *wbp2nl* mRNA as enriched in the blastomeres that primarily give rise to the ectoderm (Grant et al., 2014). In this study we assessed the developmental role of Wbp2nl using loss- and gain-of-function analyses. We show that Wbp2nl does not play a role in establishing the germ layers per se, but is involved in establishing the relative sizes of the neural plate, border zone, and epidermis territories that are derived from the embryonic ectoderm. Some of the effects in the dorsal ectoderm appear to be mediated, at least in part, by down-regulating the expression of *chd*, an anti-BMP factor. Mutation of some sites in the protein predicted by bioinformatics analyses to be functional domains revealed that the putative phosphorylation of Thr45 and the preservation of an α-helical structure in the PH-G domain are required for ectopic epidermal and neural crest gene expression in the neural plate. In contrast, a YAP-binding motif in the WWbp-domain is required only for ectopic epidermal gene expression. The various mutations had differential effects on neural plate and placode gene expression, but the frequency of *chd* repression was reduced only by mutation of the YAP binding site.

The functions of mammalian Wbp2 and Wbp2nl

Previous work showed that mammalian Wbp2nl (aka PAWP) is expressed in elongating spermatids and promotes oocyte meiotic resumption and pronucleus development at fertilization (Wu et al., 2007). These authors showed that the PPxY motif is required for pronuclear formation in oocytes from several species including *Xenopus*. They also showed that its effects on meiosis occur via the induction of intracellular calcium release (Wu et al., 2007). To our knowledge, the function of Wbp2nl after fertilization has not been investigated in any animal. Interestingly, perusal of the EMBL-EBI gene expression database (www.ebi.ac.uk) indicates that in most species (mammalian and non-mammalian), *Wbp2nl* is expressed in several adult tissues besides sperm, including kidney, heart, and brain. This

corroborates our report of expression beside sperm in the *Xenopus laevis* embryo (Grant et al., 2014), and the high levels of expression across many developmental stages reported for both *Xenopus laevis* and *X. tropicalis* on Xenbase (Yanai et al., 2011; www.xenbase.org).

Xenopus Wbp2nl is very similar to mammalian Wbp2. Mammalian Wbp2 also contains a PPxY motif that is required for binding to YAP (Chen and Sudol, 1995; Chen et al., 1997), a Hippo pathway component that modulates the transcription of many genes required for tissue-specific cell differentiation (Asaoka et al., 2014). Northern blot analysis shows that human WBP2 is expressed in multiple tissues (Chen et al., 1997), similar to the non-sperm expression of *Xenopus wbp2nl* (Grant et al., 2014; Yanai et al., 2011). The EMBL-EBI gene expression database indicates that in mouse, *Wbp2* transcripts are detected by embryonic day 14 in the adrenal gland, and later in the bone, gut, and brain (EMBL-EBI). Recent work showed that loss of *Wbp2* in mouse, and single amino acid mutations in human can lead to high-frequency hearing loss due to defects in primary afferent synapses (Buniello et al., 2016). It will be interesting to determine whether similar mutations in the highly similar *Xenopus* Wbp2nl, which is more closely related to *Homo sapiens* WBP2 protein than WBP2NL, lead to specific defects in the developing otocyst.

Does Wbp2nl play a role in BMP signaling?

Some of our results suggest that the effects on genes expressed in the dorsal ectoderm may be due to Wbp2nl down-regulating *chd*, a BMP antagonist. This is supported by the observation that providing additional Chd can abrogate the ectopic induction of epidermal and neural crest genes in the neural plate, and that there is an increase in the nuclear localization of phosphorylated SMAD1/5/8 in neural plate cells upon ectopic Wbp2nl expression. However, it is likely this is not the only mechanism by which Wbp2nl alters ectodermal gene expression. First, ectopic expression of Wbp2nl in the ventral epidermis, where BMP signaling is endogenously high, caused ectopic induction of two neural crest genes, which previous studies showed require lower BMP levels to be expressed (reviewed in Theveneau and Mayor, 2014). This suggests that in the ventral ectoderm increased Wbp2nl either interferes with BMP signaling or induces neural crest gene expression via a BMP-independent mechanism. Second, some mutations in Wbp2nl that alter its ability to ectopically induce epidermal and neural crest genes in the neural plate (T45A, F126P) do not alter its ability to down-regulate *chd*. Only the mutation that affects YAP binding (Y282F) reduced the frequency of *chd* repression. To resolve these discrepancies and to fully understand the molecular mechanisms by which Wbp2nl may modulate BMP signaling in different ectodermal contexts, a detailed analysis of the subdomains of this complex protein and dentification of the proteins with which it interacts in dorsal versus ventral ectodermal domains will be required.

Functional domains of Wbp2nl

An important feature of the Wbp2nl protein is the PH-G domain, which in other proteins is thought to bind to phosphoinositides, allow association with cell membranes and act as a stable scaffold onto which different binding functions can be imposed (Begley et al., 2003; Lemmon, 2007). We made four different mutations in the PH-G domain to discern potential functional sites. Mutation of Thr45, which is predicted to be phosphorylated by several

kinases, resulted in weaker induction of epidermal and neural crest genes, suggesting that phosphorylation of this site promotes this Wbp2nl phenotype. Mutation of Tyr55 in a putative ITSM motif, whose phosphorylation is predicted to allow interactions with SH2-containing adaptor molecules (Sidorenko and Clark, 2003), and mutation of Tyr91 in a putative STAT5 SH2 motif resulted in stronger induction of *foxD3* or *zic2*, respectively, suggesting that binding of SH2-containing proteins would dampen these phenotypes. Interestingly, mutation of each of the phosphorylation sites had only moderate effects on the repression of neural plate and placode gene expression. Since in many proteins phosphorylation of several sites in combination have the greatest impact on protein function, it will be important in future studies to mutate more than one phosphorylation site to fully discern their developmental roles. In addition to phosphorylation, we provide evidence that the 3-D structure of Wbp2nl may be of considerable functional importance. Disrupting the α-helix at the C-terminus of the PH-G domain nearly eliminated the ectopic induction of *K81, foxD3* and *zic2* in the neural plate. Thus, as predicted from its predicted complex 3D structure, the integrity of the PH-G domain is necessary for Wbp2nl to influence ectodermal gene expression.

Another conserved feature of the Wbp2nl protein is the WWbp domain. An important motif within this domain is PPxY, which in mammalian Wbp2 and Wbp2nl interacts with the Nedd4 ubiquitin-protein ligase and YAP, a mediator of Hippo signaling (Wu et al 2007; Jolliffe et al., 2000). This site is required for meiotic resumption and pronuclear formation during oocyte fertilization (Wu et al., 2007). We found that in embryos, mutation of Tyr282 within this motif prevented the ectopic induction of *K81* in the neural plate, but had only a modest effect on *foxD3* or *zic2*. Previous work showed that increasing the level of YAP in *Xenopus* embryos expands the progenitor populations in the neural plate (*sox2*) and neural border zone (*pax3*), and inhibits neural crest, PPE and epidermal genes (Gee et al., 2011). These results are opposite of the effects of increased Wbp2nl, suggesting a balance is needed between these two protein interactors.

While our analyses of the functional domains of Wbp2nl are far from complete, they demonstrate that Wbp2nl is a complex protein that contains multiple functiona sites. We demonstrate that it has a significant role in regulating the expression of several genes during the division of the embryonic ectoderm into its various neural and non-neural subdomains. Interestingly, its effects appear to be context dependent. For example, while GOF in the neural plate and in the ventral epidermis causes ectopic induction of some neural crest genes, GOF at the border zone does not expand the expression domains of these genes. Important next steps will be to elucidate all of the functional sites responsible for the effects on genes involved in subdividing the embryonic ectoderm, and how they differentially act in the different ectodermal domains.

Supplementary Material

Refer to Web version on PubMed Central for supplementary material.

Acknowledgments

We thank our many colleagues in the *Xenopus* community for providing the expression and ISH plasmids used in this study. We also thank Garrett Louie and Michael Johnson for assistance in cloning and Dr. Anastas Popratiloff (Director, GW Nanofabrication and Imaging Center) for confocal microscopy. This work would not have been possible without the support of Xenbase (http://www.xenbase.org/entry/; Karpinka et al., 2015) and the National *Xenopus* Resource (RRID:SCR_013731; Pearl et al., 2012). We acknowledge support from the NSF (MCB-1121711; SAM & DJ), NIH (R01 DE022065; SAM), GWU Dilthey Faculty Fellowship (DJ), Luther Rice Undergraduate Research Fellowship (AM), Wilbur V. Harlan Scholarship (AM) and the DC-IDDRC Cell and Tissue Microscopy Core (NIH U54 HD090257).

References

Aarabi M, Qin Z, Xu W, Mewburn J, Oko R. Sperm-borne protein, PAWP, initiates zygotic development in *Xenopus laevis* by eliciting intracellular calcium release. Mol. Repro Dev. 2010; 77:249–256.

Asaoka Y, Hata S, Namae M, Furutani-Seiki M, Nishina H. The Hippo pathway controls a switch between retinal progenitor cell proliferation and photoreceptor cell differentiation in zebrafish. PLoS One. 2014; 9:e97365. [PubMed: 24828882]

Begley MJ, Taylor GS, Kim SA, Veine DM, Dixon JE, Stuckey JA. Crystal structure of a phosphoinositide phosphatase, MTMR2: insights into myotubular myopathy and Charcot-Marie-Tooth syndrome. Mol Cell. 2003; 12:1391–402. [PubMed: 14690594]

Blum M, De Robertis EM, Wallingford JB, Niehrs C. Morpholinos: Antisense and sensibility. Dev. Cell. 2015; 35:145–149. [PubMed: 26506304]

Buchan DWA, Minneci F, Nugent TCO, Bryson K, Jones DT. Scalable web services for the PSIPRED Protein Analysis Workbench. Nucleic Acids Res. 2013; 41(W1):W340–W348. [PubMed: 23609541]

Buniello A, Ingham NJ, Lewis MA, Huma AC, Martinez-Vega R, Varela-Nieto I, Vizcay-Barrena G, Fleck RA, Houston O, Bardhan T, Johnson SL, White JK, Yuan H, Marcotti W, Steel KP. Wbp2 is required for normal glutamatergic synapses in the cochlea and is cricual for hearing. EMBO Mol. Med. 2016; 8:191–207. [PubMed: 26881968]

Chen HI, Einbond A, Kwak S-J, Linn H, Koepf E, Peterson S, Kelly JW, Sudol M. Characterization of the WW domain of human Yes-associated protein and its polyproline containing ligands. J. Biol Chem. 1997; 272:17070–17077. [PubMed: 9202023]

Chen HI, Sudol M. The WW domain of Yes-associated protein binds a proline-rich ligand that differs from the consensus established for Src homology 3-binding modules Acad. Proc. Nat. Sci. 1995; 92:7819–7823.

Dereeper A, Guignon V, Blanc G, Audic S, Buffet S, Chevenet F, Dufayard JF, Guindon S, Lefort V, Lescot M, Claverie JM, Gascuel O. Phylogeny.fr: robust phylogenetic analysis for the non-specialist. Nucleic Acids Res. 2008; 36:W465–469. [PubMed: 18424797]

Dinkel H, Van Roey K, Michael S, Kumar M, Uyar B, Altenberg B, Milchevskaya V, Schneider M, Kühn H, Behrendt A, Dahl SL, Damerell V, Diebel S, Kalman S, Klein S, Knudsen AC, Mäder C, Merrill S, Staudt A, Thiel V, Welti L, Davey NE, Diella F, Gibson TJ. ELM 2016-data update and new functionality of the eukaryotic linear motif resource. Nucleic Acids Res. 2016; 44(D1):D294–300. [PubMed: 26615199]

Edgar RC. MUSCLE: multiple sequence alignment with high accuracy and high throughput. Nucleic Acids Res. 2004; 32:1792–1797. [PubMed: 15034147]

Claros MG, Vincens P. Computational methods to predict mitochondrially imported proteins and their targeting sequences. Eur. J Biochem. 1996; 241:779–786. [PubMed: 8944766]

Gaur S, Mandelbaum M, Herold M, Majumdar HD, Neilson KM, Maynard TM, Mood K, Daar IO, Moody SA. Neural transcription factors bias cleavage stage blastomeres to give rise to neural ectoderm. genesis. 2016; 54:334–349. [PubMed: 27092474]

Gee ST, Milgram SL, Kramer KL, Conlon FL, Moody SA. Yes-associated protein 65 (YAP) expands neural progenitors and regulates Pax3 expression in the neural plate border zone. PLoS One. 2011; 6:e20309. [PubMed: 21687713]

Grant PA, Yan B, Johnson MA, Johnson DL, Moody SA. Novel animal pole-enriched maternal mRNAs are preferentially expressed in neural ectoderm. Dev Dyn. 2014; 243:478–496. [PubMed: 24155242]

Grant PA, Herold MB, Moody SA. Blastomere explants to test for cell fate commitment during embryonic development. J. Vis. Exp. Jan. 2013; 26(71):ii–4458.

Groves AK, LaBonne C. Setting appropriate boundaries: fate, patterning and competence at the neural plate border. Dev. Biol. 2014; 389:2–12. [PubMed: 24321819]

Hofmann K, Bucher P. The rsp5-domain is shared by proteins of diverse functions. FEBS letters. 1995; 358:153–157. [PubMed: 7828727]

Hong C-S, Saint-Jeannet J-P. The activity of Pax3 and Zic1 regulates three distinct cell fates at the neural plate border. Mol. Biol Cell. 2007; 18:2192–2202. [PubMed: 17409353]

Horton P, Park KJ, Obayashi T, Fujita N, Harada H, Adams-Collier CJ, Nakai K. WoLFPSORT: protein localization predictor. Nucleic Acids Res. 2007; 35W:W585–587.

Huelsenbeck JP, Ronquist F. MRBAYES: Bayesian inference of phylogenetic trees. Bioinformatics. 2001; 17:754–755. [PubMed: 11524383]

Itoh, K., Sokol, SY. Early Development of Epidermis and Neural Tissue. In: Moody, SA., editor. In Principles of Developmental Genetics. 2. New York: Academic Press; 2014. p. 189-201.

Jaurena MB, Juraver-Geslin H, Devotta A, Saint-Jeannet JP. Zic1 controls placode progenitor formation non-cell autonomously by regulating retinoic acid production and transport. Nat Commun. 2015; 6:7476. [PubMed: 26101153]

Jolliffe CN, Harvey KF, Parasivam G, Kumar S. Identification of multiple proteins expressed in murine embryos as binding partners for the WW domains of the ubiquitin-protein ligase Nedd4. Biochem J. 2000; 351:557–565. [PubMed: 11042109]

Jones DT. Protein secondary structure prediction based on position-specific scoring matrices. J. Mol Biol. 1999; 292:195–202. [PubMed: 10493868]

Karpinka JB, Fortriede JD, Burns KA, James-Zorn C, Ponferrada VG, Karimi K, Zorn AM, Vize PD. Xenbase, the *Xenopus* model organism database; new virtualized system, data types and genomes. Nucleic Acids Res. 2015; 43:D756–D763. [PubMed: 25313157]

Kelley LA, Mezolis S, Yates CM, Wass MN, Sternberg MJ. The Phyre2 web portal for protein modeling, prediction and analysis . Nat Protoc. 2015; 10:845–858. [PubMed: 25950237]

Kelley LA, Sternberg MJE. Protein structure prediction on the web: a case study using the Phyre server. Nat Protoc. 2009; 4:363–371. [PubMed: 19247286]

Klein SL. The first cleavage furrow demarcates the dorsal-ventral axis in *Xenopus* embryos. Dev Biol. 1987; 120:299–304. [PubMed: 3817297]

Klein SL, Neilson KM, Orban J, Yaklichkin S, Hoffbauer J, Mood K, Daar IO, Moody SA. Conserved structural domains in FoxD4L1, a neural forkhead box transcription factor, are required to repress or activate target genes. PLoS ONE. 2013; 8:e61845. [PubMed: 23610594]

Kosugi S, Hasebe M, Tomita M, Yanagawa H. Systematic identification of yeast cell cycle-dependent nucleocytoplasmic shuttling proteins by prediction of composite motifs. Proc. Natl. Acad. Sci. USA. 2009; 106:10171–10176. [PubMed: 19520826]

Lemmon MA. Pleckstrin homology (PH) domains and phosphoinositides . Biochem. Soc Symp. 2007; 74:81–93.

Letunic I, Doerks T, Bork P. SMART: recent updates, new developments and status in 2015. Nucleic Acids Res. 2015; 43(D1):D257–D260. [PubMed: 25300481]

Miyata S, Kageura H, Kihara HK. Regional differences of proteins in isolated cells of early embryos of Xenopus laevis. Cell Differ. 1987; 21:47–52. [PubMed: 3607883]

Moody SA, Klein SL, Karpinski BA, Maynard TM, LaMantia AS. On becoming neural: what the embryo can tell us about differentiating neural stem cells. Am. J. Stem Cells. 2013; 2:74–94. [PubMed: 23862097]

Moody, SA. Cell lineage analysis in *Xenopus* embryos. In: Tuan, RS., Lo, CW., editors. Methods in Molecular Biology: Developmental Biology Protocols. Vol. 135. Humana Press; 2000. p. 1-17.

Moody SA. Fates of the blastomeres of the 16-cell stage *Xenopus* embryo. Dev. Biol. 1987; 119:560–578. [PubMed: 3803718]

Moody SA, Kline MJ. Segregation of fate during cleavage of frog (*Xenopus laevis*) blastomeres. Anatomy & Embryology. 1990; 182:347–362. [PubMed: 2252221]

Neilson KM, Klein SL, Mhaske P, Mood K, Daar IO, Moody SA. Specific domains of FoxD4/5 activate and repress neural transcription factor genes to control the progression of immature neural ectoderm to differentiating neural plate. Dev. Biol. 2012; 365:363–375. [PubMed: 22425621]

Nieuwkoop, PD., Faber, J. Normal Table of *Xenopus laevis* (Daudin). Garland Publishing Inc.; New York: 1994.

Nguyen Ba AN, Pogoutse A, Provart N, Moses A. NLStradamus: a simple Hidden Markov Model for nuclear localization signal prediction. BMC Bioinformatics. 2009; 10:202. [PubMed: 19563654]

Pearl EJ, Grainger RM, Guile M, Horb ME. Development of *Xenopus* resource centers: the National Xenopus Resource and the European *Xenopus* Resource Center. genesis. 50:155–163.

Pollastri G, McLysaght A. Porter: a new, accurate server for protein secondary structure prediction. Bioinformatics. 2005; 21:1719–1720. [PubMed: 15585524]

Salah Z, Alian A, Aqeilan RI. WW domain-containing proteins: retrospectives and the future. Front Biosci. 2012; 17:331–348.

Sidorenko SP, Clark EA. The dual-function CD150 receptor subfamily: the viral attraction. Nat Immunol. 2003; 4:19–24. [PubMed: 12496974]

Sievers F, Wilm A, Dineen D, Gibson TJ, Karplus K, Li W, Lopez R, McWIllaim H, Remmert M, Soding J, Thompson JD, Higgins DG. Fast, scalable generation of high-quality protein multiple sequence alignmnets using Clustal Omega. Molec. Syst Biol. 2011; 7:539. [PubMed: 21988835]

Sudol M. WW domains in the heart of Smad regulation. Structure. 2012; 20:619–1620.

Sudol M, Sliwa K, Russo T. Functions of WW domains in the nucleus. FEBS Letters. 2001; 490:190–195. [PubMed: 11223034]

Sullivan SA, Akers L, Moody SA. foxD5a, a *Xenopus* winged helix gene, maintains an immature neural ectoderm via transcriptional repression that is dependent on the C-terminal domain. Dev Biol. 2001; 232:439–457. [PubMed: 11401404]

Theveneau, E., Mayor, R. Neural Crest Determination and Migration. In: Moody, SA., editor. In Principles of Developmental Genetics. 2. New York: Academic Press; 2014. p. 315-330.

Wu AT, Sutovsky P, Manandhar G, Xu W, Katayama M, Day BN, Park KW, Yi YJ, Xi YW, Prather RS, et al. PAWP, a sperm-specific WW domain-binding protein, promotes meiotic resumption and pronuclear development during fertilization. J. Biol Chem. 2007; 282:12164–12175. [PubMed: 17289678]

Xavier R, Gouet P. Deciphering key features in protein structures with the new end script server. Nucleic Acids Res. 2014; 42(W1):W320–W324. [PubMed: 24753421]

Yan B, Neilson KM, Moody SA. FoxD5 plays a critical upstream role in regulating neural fate and onset of differentiation. Dev Biol. 2009; 329:80–95. [PubMed: 19250931]

Yanai I, Peshkin L, Jorgensen P, Kirschner MW. Mapping gene expression in two Xenopus species: evolutionary constraints and developmental flexibility. Dev. Cell. 2011; 20:483–496. [PubMed: 21497761]

Zhang C, Klymkowsky MW. The Sox axis, Nodal signaling, and germ layer specification. Differentiation. 2007; 75:536–545. [PubMed: 17608734]

Highlights

- Wbp2nl helps establish the size of neural plate, border zone and epidermis domains
- Its effects in dorsal ectoderm are partially mediated by regulating *chd* expression
- Thr45 phosphorylation is required for ectopic epidermal and neural crest expression
- An α-helix in the PH-G domain also is required for these activities
- A YAP-binding motif is required for ectopic *K81* expression and *chd* repression

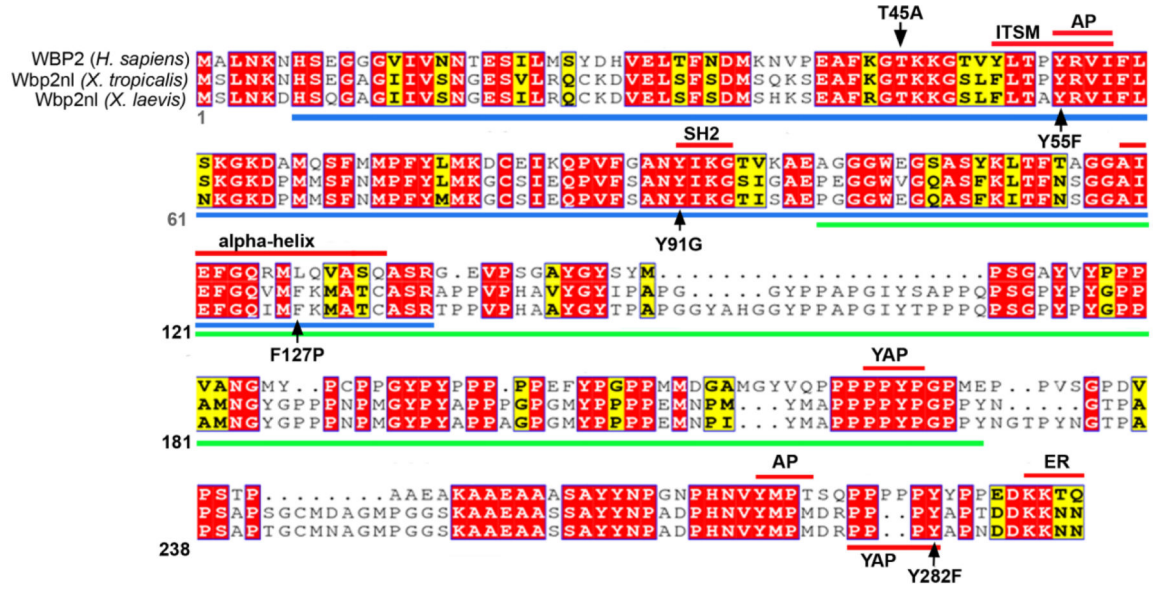

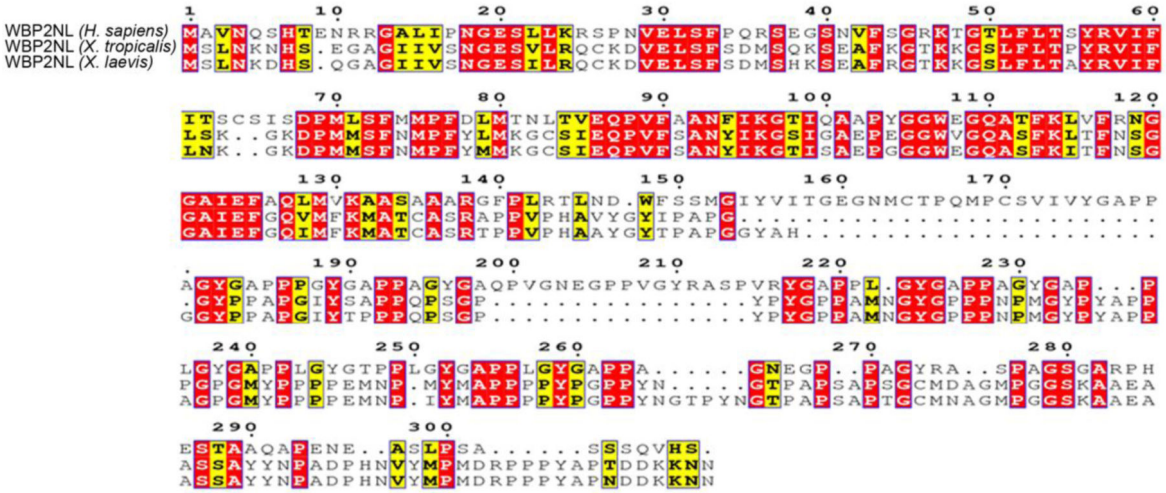

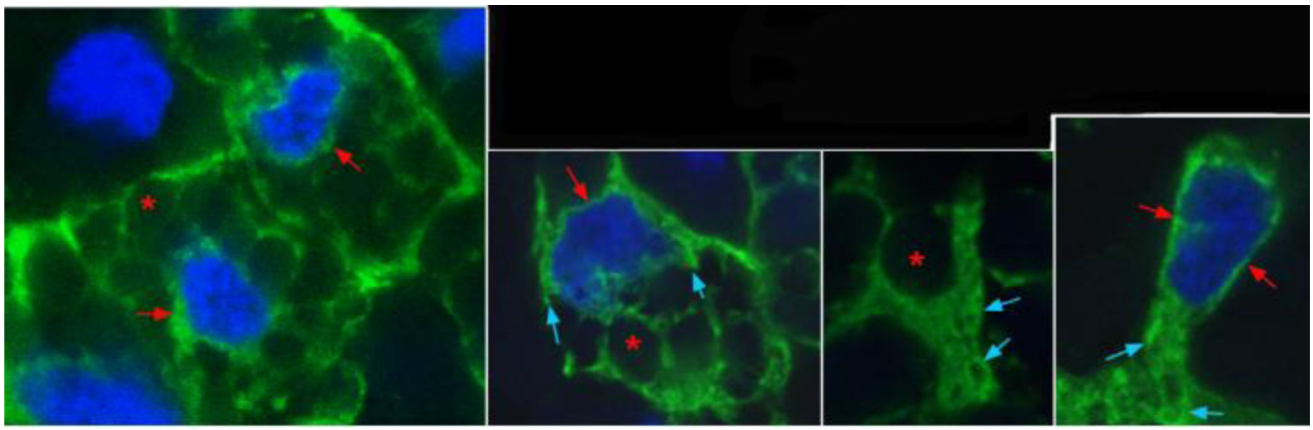

Figure 1. Amino acid sequence alignments of *Xenopus* Wbp2nl to human WBP2 and WBP2NL

(A) *Xenopus* Wbp2nl (NP_001088037.1 *[laevis]* and NP_001107397.1 *[tropicalis]*) is highly similar to human WBP2 (NP_036610.2). Blue bar indicates the predicted PH-G domain and green bar indicates the predicted WWbp domain. Highly conserved motifs and α-helix are indicated by red bars. Five single amino acid mutations that were experimentally tested for function are indicated by black arrows (T45A, Y55F, Y91G, F127P, Y282F). AP, adaptor protein complex; ER, endoplasmic reticulum retention signal; ITSM, immunoreceptor tyrosine-based switch motif; SH2, Scr Homology domain 2; YAP, Yes associated protein binding motif. **(B)** Comparison of human WBP2NL (AAH22546.1) to *Xenopus* sequences shows large regions of disimilarity. Another human WBP2NL entry (Q6ICG8.1) is identical to AAH22546.1 except there is a glutamine at position 285 instead of a histidine. **(C)** Four examples of cells immunostained for Myc-Wbp2nl (green). Nuclei are stained with DAPI (blue). Note that staining is perinuclear (red arrows, and in cytoplasmic tubular structures (blue arrows) consistent with affiliation with Endoplasmic reticulum. Red asterisks denote intracellular yolk platelets.

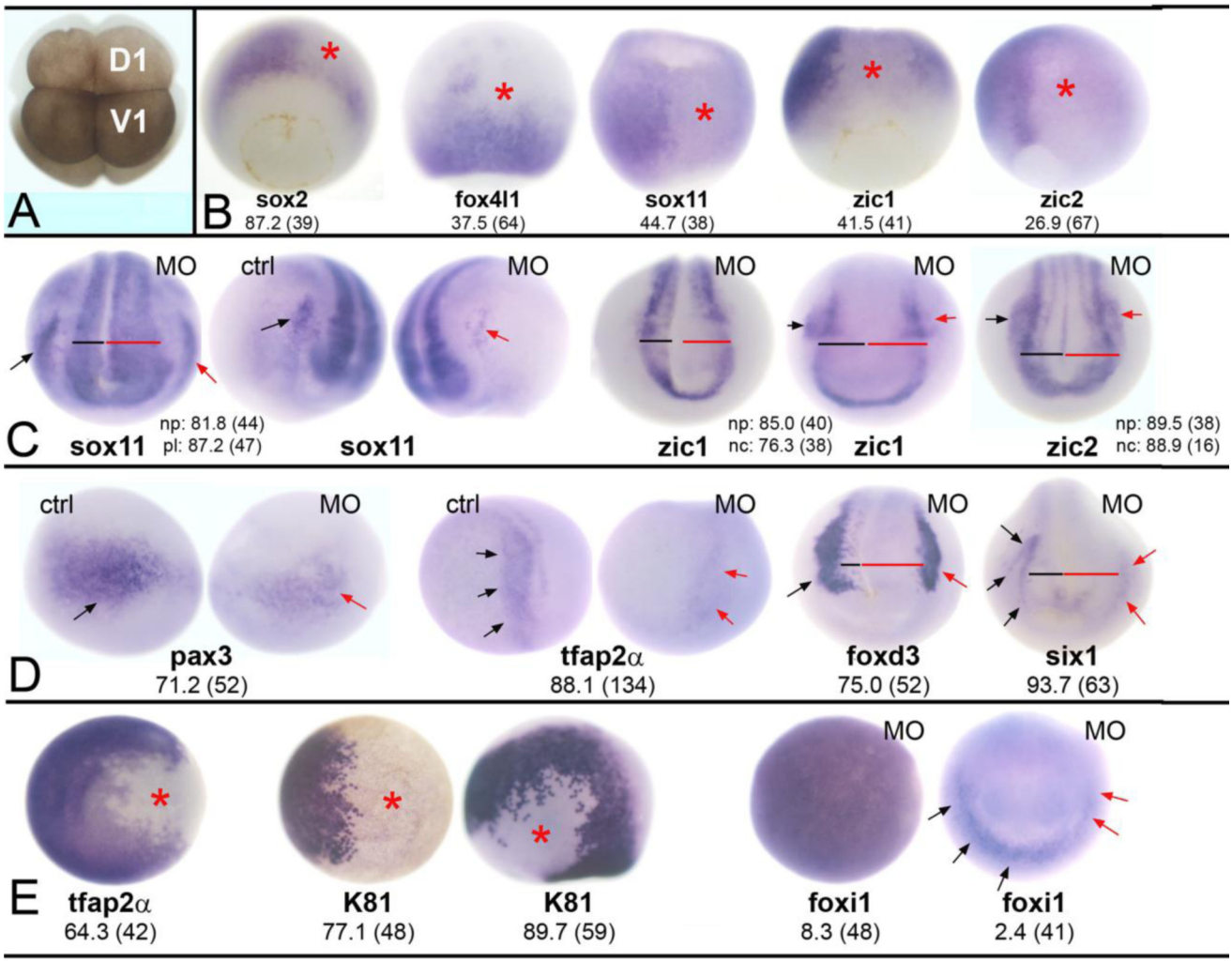

Figure 2. Reduction of Wbp2nl affects ectodermal tissues

(**A**) An 8-cell *Xenopus laevis* embryo. The dorsal-animal blastomere (D1) gives rise to the neural plate and the ventral-animal blastomere (V1) gives rise to the epidermis. Border zone derivatives (neural crest and cranial placodes) descend from the lateral regions of both blastomeres (Moody and Kline, 1990). (**B**) Knock-down of Wbp2nl causes a decrease in the expression (loss of blue reaction product) of neural ectodermal genes on the MO-injected side (asterisk) of gastrula stage embryos. *sox2* is a vegetal view with dorsal to the top; the rest are dorsal views with animal to the top. (**C**) By neural plate stages, neural gene domains are expanded; compare the width of the neural plate on MO-injected side (red bar) to control side (black bar). (See also **D**). The PPE domains of *sox11* and the neural crest domains of *zic1* and *zic2* are reduced on MO-injected sides (red arrows) compared to control sides (black arrows). Anterior views with dorsal to the top. (**D**) At neural plate stages, neural crest markers (*pax3, tfap2α, foxd3*) and an early PPE marker (*six1*) are reduced on the MO-injected side (red arrows) compared to control sides (black arrows). Also note wider neural plates (red bars). *pax3* and *tfap2α* are anterior-side views; *foxd3* and *six1* are anterior views. (**E**) Two epidermal genes are reduced at the sites of Wbp2nl knock-down (asterisks) at gastrula (*tfap2α, K81* right image; both are animal pole views) and neural plate (*K81* left

image; side view with dorsal to top and anterior to right) stages. In contrast, the animal pole expression of *foxi1* in the gastrula (left image) is not altered. Rarely, the PPE expression of *foxi1* (right image; anterior view with dorsal to top) is reduced (red arrows) after Wbp2nl knockdown. Frequencies of the phenotypes and sample sizes (n) are given in each panel.

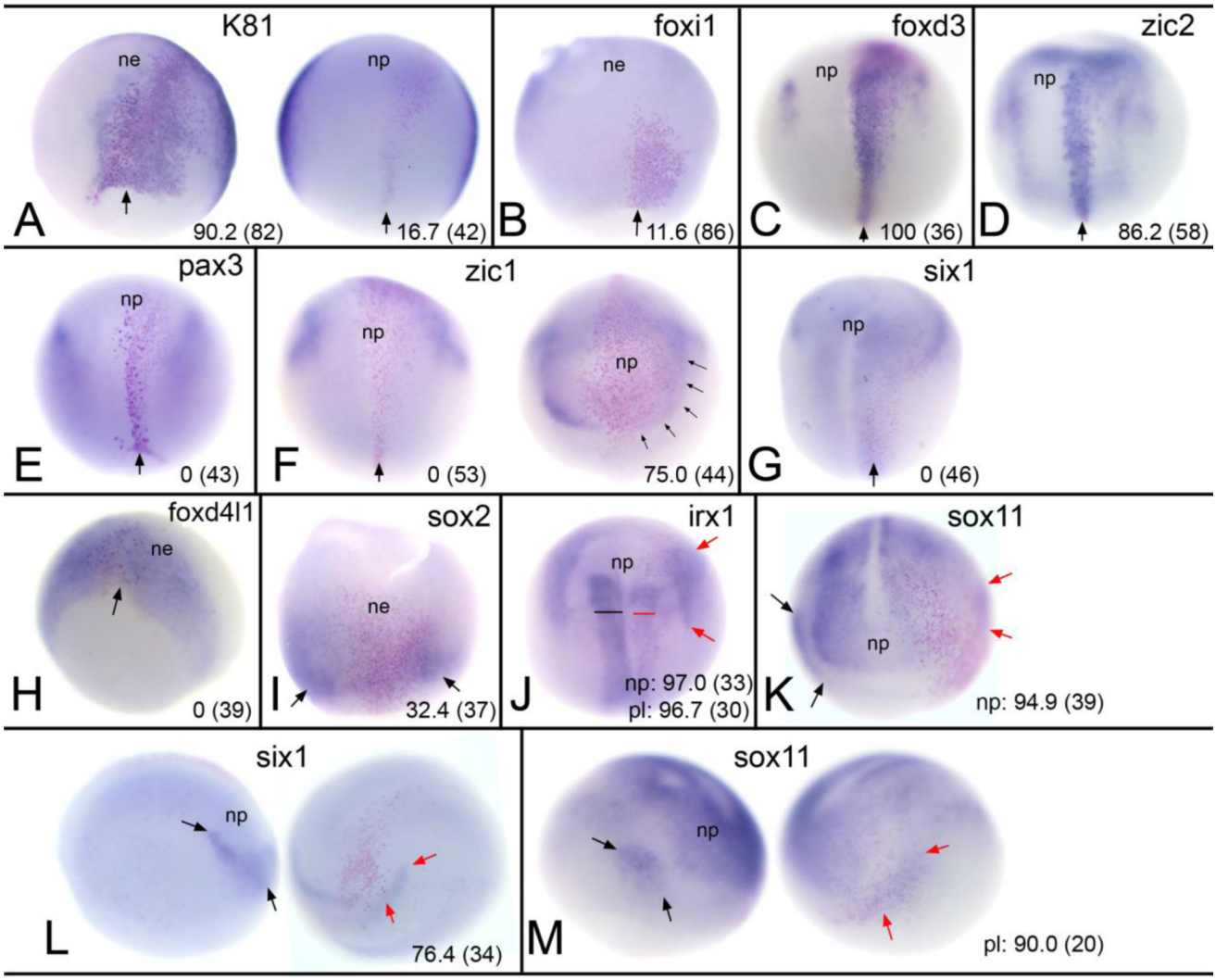

Figure 3. Increasing Wbp2nl levels alters ectodermal gene expression

(A) Increased Wbp2nl causes ectopic expression of epidermal keratin (*K81*) in the neural ectoderm (ne) at gastrula stages (left) but not at neural plate (np) stages (right). Pink nuclei identify the cells that are expressing excess Wbp2nl and the black arrow indicated the posterior extent of the clone. A–D, dorsal views with animal to top. **(B)** Increased Wbp2nl does not induce ectopic *foxi1* in the ne. **(C)** Increased Wbp2nl causes ectopic expression of *foxd3* in the neural plate (np). **(D)** Increased Wbp2nl causes ectopic expression of *zic2* in the neural plate. **(E–G)** Increased Wbp2nl does not cause ectopic neural plate expression of *pax3, zic1* or *six1* (dorsal views with animal to top). In fact, *zic1* neural plate expression is reduced on the injected side (**F**, right image, anterior view, dorsal to top). **(H)** Increased Wbp2nl does not alter *foxd4l1* neural ectoderm expression. Vegetal-dorsal view. **(I)** Neural ectoderm expression of *sox2* in the gastrula is reduced compared to lateral regions (black arrows) that do not contain Wbp2nl-expressing cells (pink nuclei). Dorsal view, animal to top. **(J)** Both the neural plate (red bar) and placode (red arrows) domains of *irx1* are reduced by increased Wbp2nl compared to control side (black bar). Dorsal view, anterior to top. **(K)** Both the neural plate and placode (red arrows) expression of *sox11* are reduced by increased

Wbp2nl. Anterior view, dorsal to top. **(L)** The placode (red arrows) domain of *six1* is reduced by increased Wbp2nl, compared to control uninjected side (black arrows). Side views, dorsal to top. **(M)** The placode (red arrows) domain of *sox11* is reduced by increased Wbp2nl compared to control uninjected side (black arrows). Note reduced neural plate (np) staining as well. Side views, dorsal to top. Frequencies of the phenotypes and sample sizes (n) are given in each panel.

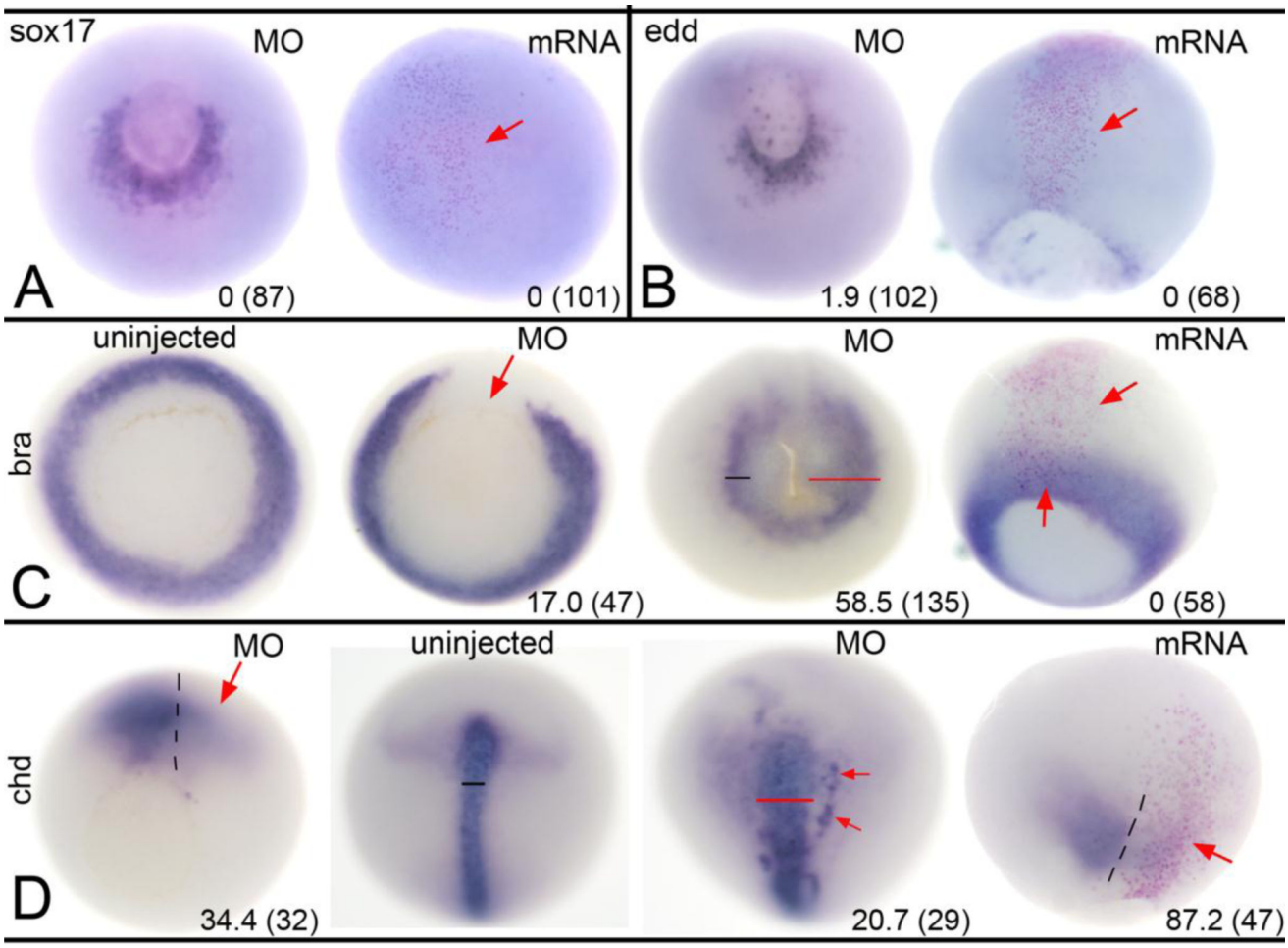

Figure 4. Altered Wbp2nl levels affect mesoderm but not endoderm

(A) At gastrula stages, *sox17* expression surrounding the ventral blastopore on the MO-injected side of an embryo (left image, vegetal view) is not discernably different from control side. Increased Wbp2nl in the animal pole ectoderm (right image, animal view; clone marked by pink nuclei and red arrow) does not ectopically induce *sox17*. **(B)** At gastrula stages, *edd* expression surrounding the ventral blastopore on the MO-injected side (left image, vegetal view) is not discernably different from control side. Increased Wbp2nl in the neural ectoderm (right image, dorsal view; clone marked by pink nuclei and red arrow) does not ectopically induce *edd*. **(C)** At gastrula stages, mesoderm expression of *bra* encircles the blastopore in uninjected control embryos (left image, vegetal view); knockdown of Wbp2nl causes a loss of *bra* expression (left middle image, vegetal view, red arrow). In contrast, at neural plate stages (right middle image, vegetal view), we detect a posterior expansion (red bar) of bra expression on the knock-down side. At gastrula stages, increased Wbp2nl (right image, dorsal view; clone marked by pink nuclei between red arrows) does not alter endogenous *bra* expression nor ectopically induce it. **(D)** At gastrula stages, mesoderm expression of *chd* is reduced by Wbp2nl knock-down (red arrow, left image, vegetal view; dashed line indicates dorsal midline). In contrast, at neural plate stages, *chd* is expanded (compare uninjected control pattern [left middle image] to MO-injected pattern [right middle image]; dorsal views with anterior to the top). Red bar shows a wider domain and red arrows

denote ectopic expression. At gastrula stages, increased Wbp2nl (right image, dorsal view, anterior to top; dashed line indicates dorsal midline) also reduces endogenous *chd* expression (red arrow). Frequencies of the phenotypes and sample sizes (n) are given in each panel.

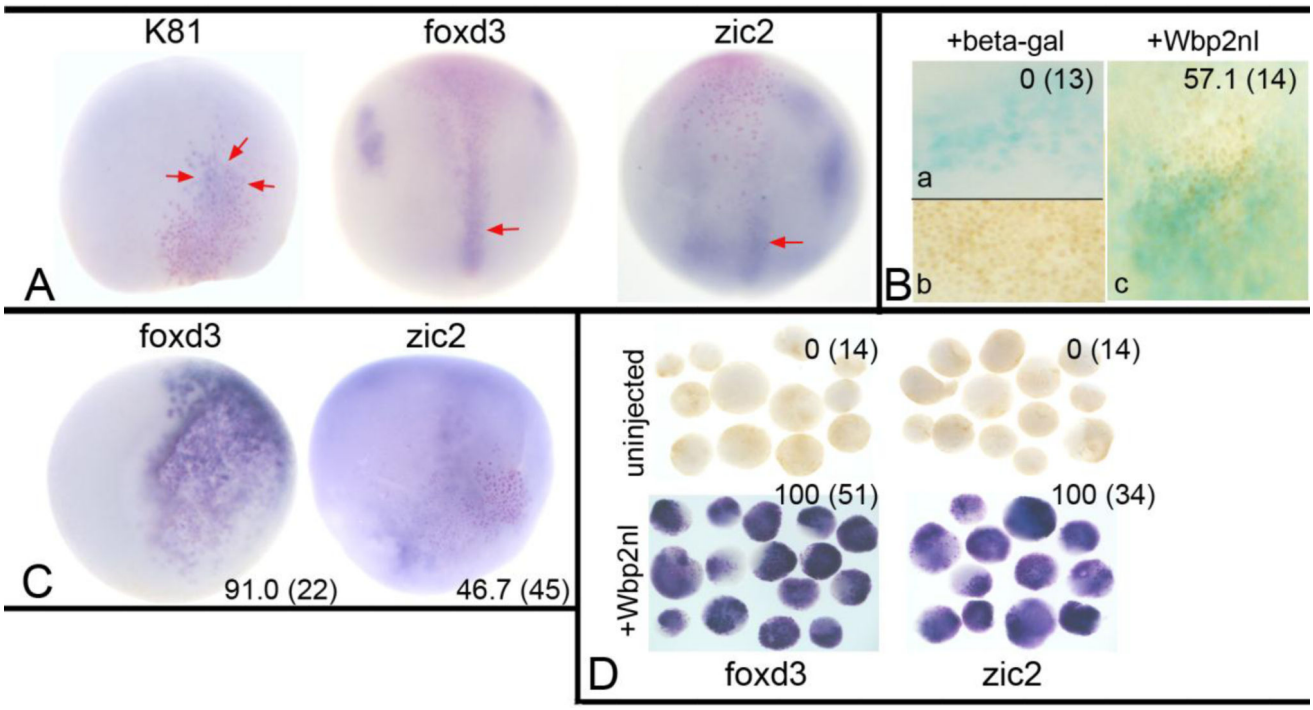

Figure 5. BMP signaling underlies Wbp2nl-induced ectopic expression phenotypes

(A) The ectopic expression of *K81, foxd3* and *zic2* are minimized by co-expression of Chd, a BMP antagonist. Red arrows point to weak posterior ectopic gene expression observed in those few embryos that were positively scored. **(B)** Immunostaining for phosphorylated SMAD 1/5/8, an indicator of BMP signaling when located in the nucleus. Only embryos in which ventral cells, which are subject to high levels of endogenous BMP signaling, showed nuclear staining were analyzed (b). No embryo injected only with lineage tracer (blue) showed nuclear staining in the neural plate (a), whereas a majority of embryos injected with lineage tracer plus *wbp2nl* mRNA showed nuclear staining (c). **(C)** Expression of Wbp2nl in the ventral epidermis causes ectopic expression of two neural crest genes (*foxd3, zic2*). Pink nuclei (lineage tracer) indicate the Wbp2nl containing cells. Ventral views, anterior to the top. **(D)** Ventral animal blastomeres were dissected from the 16-cell stage embryo and cultured in simple salt medium. Those dissected from uninjected control embryos never expressed *foxd3* or *zic2*, whereas those that express Wbp2nl (red nuclei) always expressed these genes. Frequencies of the phenotypes and sample sizes (n) are given in each panel.

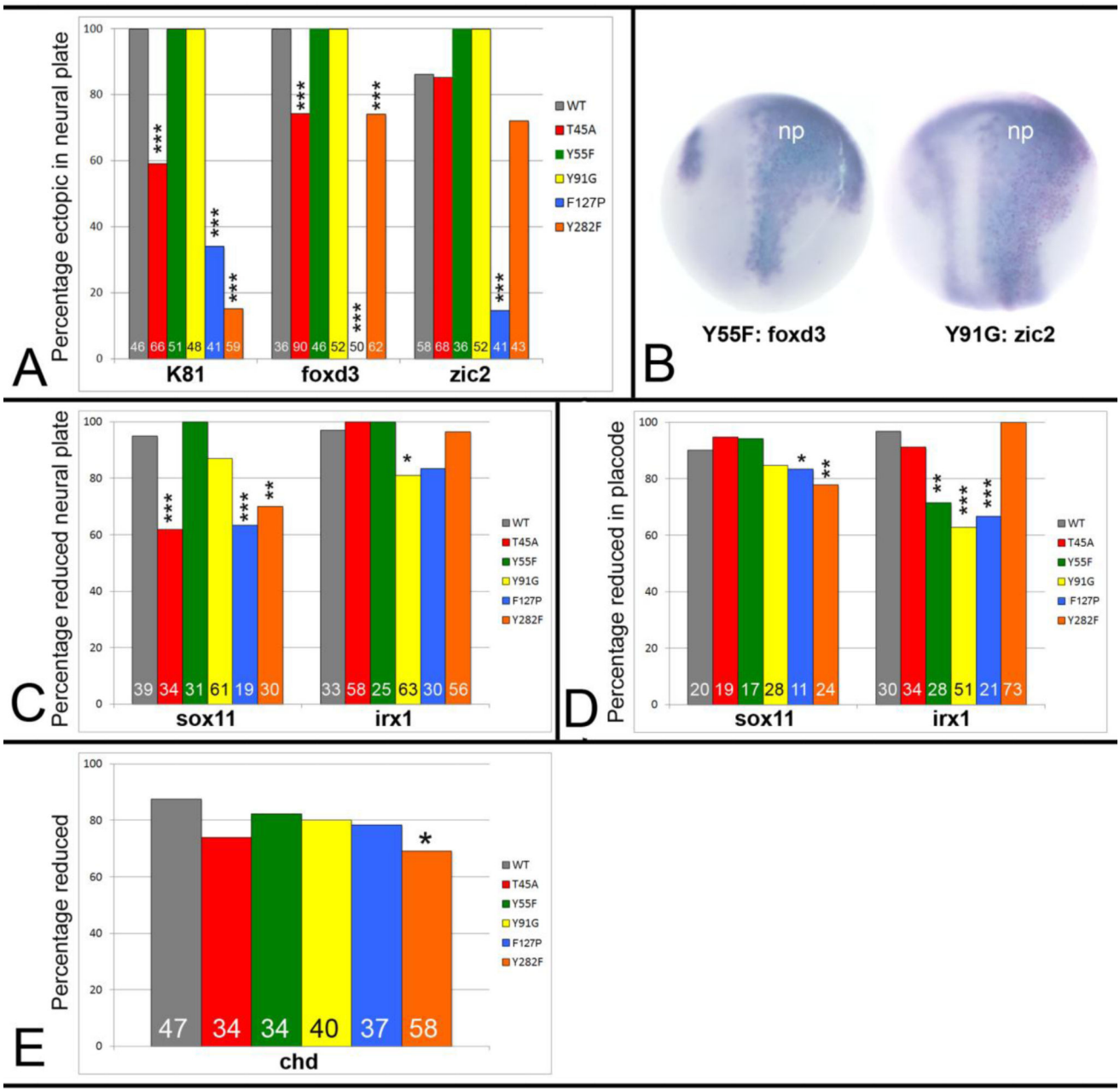

Figure 6. Mutations in predicted functional domains of Wbp2nl, indicated in Figure 1A, affect its ability to change embryonic gene expression

(A) Percentages of embryos that show ectopic neural plate expression of indicated genes after injection of wild type (WT) or mutated mRNAs: T45A, Y55F and Y91G disrupt putative phosphorylation sites in the PH-G domain; F127P disrupts an a-helix in the PH-G domain; Y282F disrupts a putative YAP binding site at the C-terminus (see Figure 1A). Sample sizes are numbers at the base of each bar. *, p<0.05; **, p<0.01; ***, p<0.005, Chi-squared statistic. **(B)** Two examples of more intense and broader ectopic expression domains of *foxd3* or *zic2* in the neural plate (np) after expression of two mutant proteins (Y55F; Y91G). Compare to WT images (Fig. 4C, D). Dorsal views, anterior to the top. **(C)**

Percentages of embryos that show reduced neural plate expression of indicated genes after expression of wild type (WT) or mutated proteins. **(D)** Percentages of embryos that show reduced placode expression of indicated genes after expression of wild type (WT) or mutated proteins. **(E)** Percentages of embryos that show reduced *chd* expression after expression of wild type (WT) or mutated proteins.